The major asperities of the 1999 $M_w = 7.4$ Izmit earthquake defined by the microseismicity of the two decades before it

Ali Osman Öncel[1] and Max Wyss[2]

[1] *Department of Geophysical Engineering, University of İstanbul, Avcılar-Istanbul 34850, Turkey. E-mail: oncel@hotmail.com*
[2] *Geophysical Institute, University of Alaska, Fairbanks, AK 99775, USA. E-mail: max@giseis.alaska.edu.*

SUMMARY

We compare the rupture location of the M_w 7.4 Izmit earthquake to the local seismic hazard estimated by the technique of mapping local recurrence time, T_L, based on the microseismicity. After correcting for a magnitude shift in 1990, the declustered earthquake catalogue, produced by the University of Istanbul for the Marmara Sea region, is homogeneous for $M_d \geq 2.9$ during 1983–1999. We mapped T_L in the area bounded by 40°–41° latitude and 27.6°–30.5° longitude. T_L is the probabilistic estimate of recurrence time, calculated from the *a*- and *b*-values of the frequency–magnitude relation of the seismicity within a radius of 20 km from every point on a grid with 5 km spacing. T_L varies strongly as a function of space, since *a*- and *b*-values also vary strongly. In our interpretation, the 5–20 per cent of locations with the shortest recurrence times map major asperities. In the Marmara region, we mapped four anomalies of short T_L, together covering about 12 per cent of the total area. They are centred near 40.25°/29.4°, 40.8°/28.3°, 40.75°/28.8° and 40.7°/29.8°. The last two of these coincide with the western end of the rupture and the epicentre location of the Izmit earthquake, respectively. Thus, we suggest that the major asperity of this rupture and a point past which it could not propagate were mapped out by the background seismicity during the years before the event as locations that produced more large microearthquakes than average, and hence showed anomalously short T_L. The T_L method does not contain information about when earthquakes are expected, and the absolute values of the recurrence time could be inaccurate. The method only specifies the most likely locations of main shocks. Since the method is new, it will have to be tested for many cases and in many areas before its reliability can be assessed.

Key words: *b*-values, earthquake prediction, fault models, seismicity.

INTRODUCTION

Recently, the technique of mapping local recurrence time $[T_L(M)]$ was successfully used to estimate locations of asperities based on the earthquakes within r = constant of the location in question ($5 \leq r \leq 20$ km) (Wiemer & Wyss 1997; Wyss *et al.* 2000; Zuniga & Wyss 2000). T_L can be estimated from the parameters of log-linear scaling,

$$\log N = a - bM , \qquad (1)$$

where N is the number of earthquakes with magnitude M and larger over the observation period dT, by

$$T_L(M) = dT/10^{(a-bM)} . \qquad (2)$$

Wiemer & Wyss (1997) argued that asperities are the only segments of faults that may contain information about the frequency of ruptures in main shocks because they control the

time of rupture. For this reason, the recurrence time should be mapped as a local parameter. Bulk values of recurrence time, derived from asperities plus passive fault segments that slide along with the asperity when the latter ruptures, are incorrect according to this hypothesis.

Size scaling parameters of seismicity (*a* and *b*) in the space and time domains can be affected by several physical factors such as material heterogeneity and applied shear stress level (Mogi 1962; Scholz 1968; Wyss 1973; Urbancic *et al.* 1992) and thermal gradient (Warren & Latham 1970). However, only recently has it become clear that *b* also varies strongly with the clustering degree of seismicity and fracture (e.g. Öncel *et al.* 1995, 1996a,b, 1999) over distances of a few kilometres (Ogata & Katsura 1993; Wiemer & Benoit 1996; Wiemer & McNutt 1997; Wiemer & Wyss 1997), although the average *b*-value in large volumes tends to show constant values near 1 (Frohlich & Davis 1993; Kagan & Jackson 1991).

The creeping part of the San Andreas fault north of Parkfield shows anomalously high *b*-values (Amelung & King 1997; Wiemer & Wyss 1997), whereas the segment beneath Middle Mountain, which is known as an asperity, shows the lowest *b*-values in the 150 km long fault segment that it is included in (Wiemer & Wyss 1997). In addition, the asperities of the Morgan Hill *M*6 earthquake (Wiemer & Wyss 1997) and the Anza seismic gap in the San Jacinto fault zone (Wyss *et al.* 2000) are locations of anomalously low *b*-values. These anomalies become even more pronounced in maps of T_L, where they constitute about 10 per cent of the area mapped and where T_L is substantially shorter than in other fault segments.

Thus, in this paper we further investigate the possibility that local changes of $T_L(M)$ are related to the rate of activity (*a*-parameter) and stress (*b*-parameter) and may be used to map asperities. We define an asperity as a segment of a fault plane resisting faulting more than its surroundings, as it is generally defined in models for earthquake rupture (e.g. Wyss & Brune 1967; Lay *et al.* 1982; Aki 1984). The bulk *a*- and *b*-values of the main-shock rupture areas often lead to overestimates of the recurrence time for main shocks, whereas the asperities are found to exhibit the lowest values of *b* ($b \approx 0.5$) and the lowest T_L, which agree better with historically observed recurrence times (Wiemer & Wyss 1997; Öncel & Alptekin 1999a).

The most important aspect of our mapping of T_L is the *contrast* between the <10 per cent of the area that shows anomalously short recurrence times and the rest of the area. The absolute values of the recurrence time are only of secondary interest because they may not be very reliable at this stage of our understanding of the problem. The model for short T_L anomalies that we have in mind is as follows. Fault segments with anomalously short T_L are relatively active segments in which the mean magnitude resulting from fractures is larger than along the rest of the fault. Thus, these segments are singled out as having different physical properties, and we propose that they are asperities. These asperities control the time of rupture, and surrounding segments of lower strength rupture along with the asperities relatively passively. As strong spots, the asperities can inhibit rupture propagation when they are not highly loaded with stress, but once they are loaded, their rupture leads to a major earthquake. The rupture of such a major earthquake is most likely to initiate within an asperity, but it can also happen that a rupture that is initiated outside but near the asperity propagates into the asperity and triggers the event. In our hypothesis, the asperities do not contain information on the maximum size to which a rupture involving an asperity may grow. The minimum magnitude is given by the area of the asperity itself as the earthquake that would result if the rupture stopped at the edge of the asperity. However, the maximum magnitude is unknown, because the rupture can reach another asperity and beyond this yet another asperity that is loaded with stress.

Based on this model, we expect that a major asperity should be located at or near the epicentre (rupture initiation) of large earthquakes. Also, large ruptures probably, but not necessarily, end at asperities. Finally, one or several additional asperities may be located within a multiple-event rupture of a large earthquake. Although a great earthquake might be generated by connecting a large number of moderate-size asperities, it is probable that the maximum size of asperities scales in most cases approximately with the largest main shock a fault is capable of. In a preliminary investigation we found that the ratio of the length of a main shock to the length of its major asperity is about 4:1 (Wyss *et al.* 2000). Thus, we estimate that the size of major asperities in the case of the Izmit earthquake may be about 25 km. To map such features sharply, it would be desirable to have a data density that would allow sampling with radii of 10 km. However, mapping T_L anomalies corresponding to the expected asperity size using larger radii for sampling ($r = 20$ km, as we are forced to use here) is still possible, although not optimal.

The seismicity of the Marmara Sea region is strongly related to the tectonic characteristics of the North Anatolian Fault Zone (NAFZ) (Crampin & Üçer 1975; Öncel & Alptekin 1995). This region is located in a transition zone between Eurasia and NW Anatolia (Straub & Kahle 1995). Details of the fault geometry associated with large destructive earthquakes along the NAFZ and their relationship to spatial and temporal patterns of seismic clustering are not well understood (Ambraseys & Finkel 1991). The comprehensive evaluation of spatial attributes of earthquake clustering in this region may define the evolution of asperities and provide important information relevant to earthquake hazard assessment for cities such as Istanbul in the Marmara Sea Region. The main purposes of this paper are (1) to evaluate the size scaling parameters of seismicity (*a* and *b*) in the Marmara Sea region, and (2) to determine local variations of earthquake recurrence correlating in some way with the locations of asperities, which might indicate potential rupture initiation or termination in future large earthquakes.

DATA

The raw earthquake catalogue was compiled by the Kandilli Observatory and the Earthquake Research Institute (KOERI), augmented by the Turkish national network and by local seismic networks, with good station coverage, particularly since 1970 (Öncel *et al.* 1995). The map of seismicity in Fig. 1 indicates that the regional seismicity is controlled by strong clusters along the Marmara Sea region, especially at the location where the recent Izmit earthquake occurred in the eastern part of the region. The frequency–magnitude relation in Fig. 2 shows that the data are complete for events with $M_d \geq 2.9$.

After declustering using the algorithm of Reasenberg (1985) programmed in ZMAP (Wiemer 1996) and correcting for a magnitude shift in 1990, the cumulative number of earthquakes reported in the catalogue for the Marmara Sea region (http://www.angelfire.com/al/geophysics) (Öncel & Alptekin 1999b) shows a constant slope with time (Fig. 3). We interpret this to mean that the reporting was homogeneous since 1983, if the magnitude correction is applied.

MAPPING *b*-VALUES AND LOCAL RECURRENCE TIME

For mapping *b* and T_L we use spatial subdivisions along the Marmara Sea (Fig. 1) consisting of fixed cylindrical volumes with radius *r* equal to 20 km and height *h* equal to 40 km. The centres of the cylindrical volumes are positioned at nodes with a 5 km spacing throughout the region. The parameters *a* and *b* are then estimated from the events with $M \geq M_c$ for each volume by the gridding technique introduced by Wiemer (1996). Mapping of $T_L(M)$ from the resulting matrix of *a*- and *b*-values can be computed from eq. (2) for a given magnitude of the
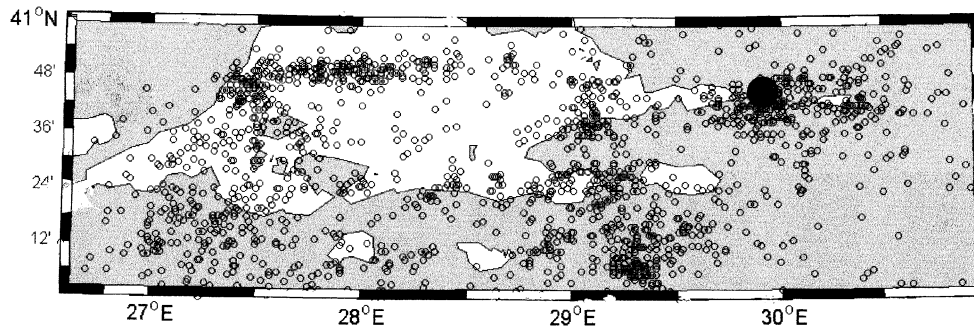
Figure 1. Epicentre map of the Marmara Sea region for earthquakes with $M \geq 2.9$ between 1983 and 1998.

expected main shock. All of the computations are programmed in zMAP, a computer code introduced by Wiemer (1996) and expanded continuously since by Wiemer.

The *b*-value map, resulting from the procedure outlined above for the Marmara Sea in NW Turkey, is shown in Fig. 4(a). One can see that, on average, $b = 1.3$, but locally the values range from 0.9 to 1.6. Clearly, a strong heterogeneity of *b*-values exists in the region. The *a*-value map in Fig. 4(b) shows the varying activity in the region.

The map of local recurrence time (Fig. 4c) calculated from eq. (2) is based on a main-shock magnitude of the same scale as the earthquake catalogue. This is the M_D scale, on which the Izmit $M_w = 7.4$ earthquake measures $M_D = 6.7$ according to the Kandilli observatory.

The T_L map shows similar patterns to the *b*-value map, but it sharpens the contrasts. We identify four areas of anomalously low T_L. (1) Area I, a segment along Izmit bay, between 29.5° and 30.0° longitude, is located adjacent to the moment centroid epicentre. In this area, T_L is estimated as about 1000–1500 yr. (2) Area II, a segment of strongly anomalous T_L, coincides with the westernmost end of the 1999 Izmit rupture. (3) Area III, located at longitude 28.3° along the northern branch of the north Anatolian fault, is a weaker anomaly with estimates of about 500–1500 yr for T_L. (4) Area IV is located between longitudes 29.0° and 29.5° and has the shortest T_L estimate of about

500 yr. It coincides with the largest earthquake in the catalogue during the 17 years before the Izmit earthquake of August 1999.

DISCUSSION AND CONCLUSIONS

Recently, the question has been discussed whether the background seismicity during times between main shocks could provide clues about the location of past and future main shocks (Wyss *et al.* 1999). The occurrence of the M_s 7.4 Izmit earthquake allows us to test whether the mapping of anomalous areas by the T_L technique can identify asperities that may play a key role in ruptures along the NAFZ. The Marmara Sea region is one of the seismically best monitored parts of Turkey, thus the data allow a relatively detailed mapping of T_L. During the period of the modern earthquake catalogue (1983–1999), no earthquakes with $M \geq 5.6$ occurred, hence no such events or their aftershock sequences contaminate the *b*- and *a*-value data. Thus, the data set available is adequate for determining
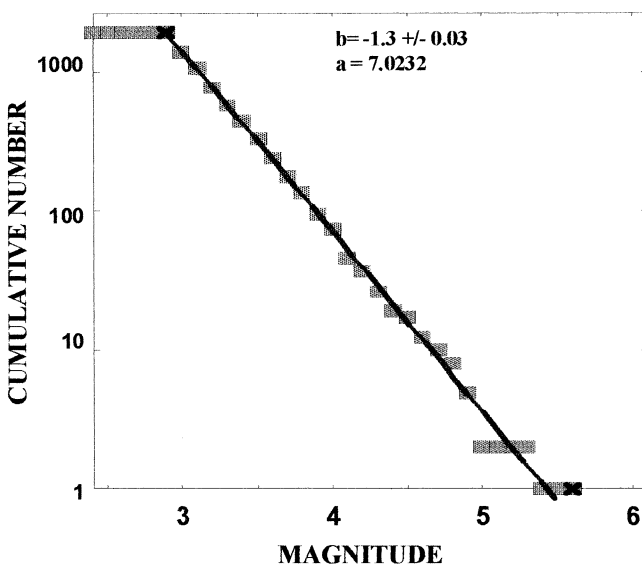

Figure 2. Cumulative number of earthquakes, excluding clusters, as a function of magnitude for the Marmara Sea region during the period 1983–1998 ($M_D \geq 2.9$.) The minimum magnitude of completeness is 2.9.
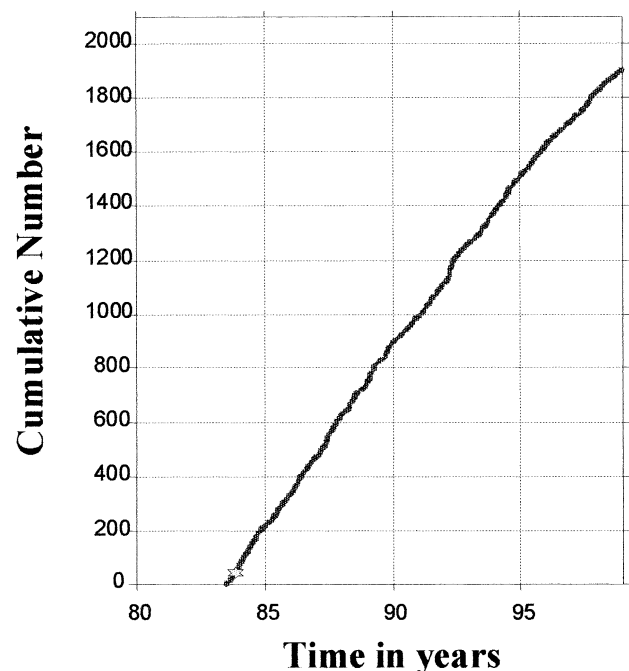

Figure 3. Cumulative number of earthquakes with magnitude of $M_D \geq 2.9$ as a function of time for the Marmara Sea region, corrected for a magnitude shift of $dM = 0.3$ in 1990. The relatively constant and smooth slope suggests that this catalogue can be accepted as homogeneous.
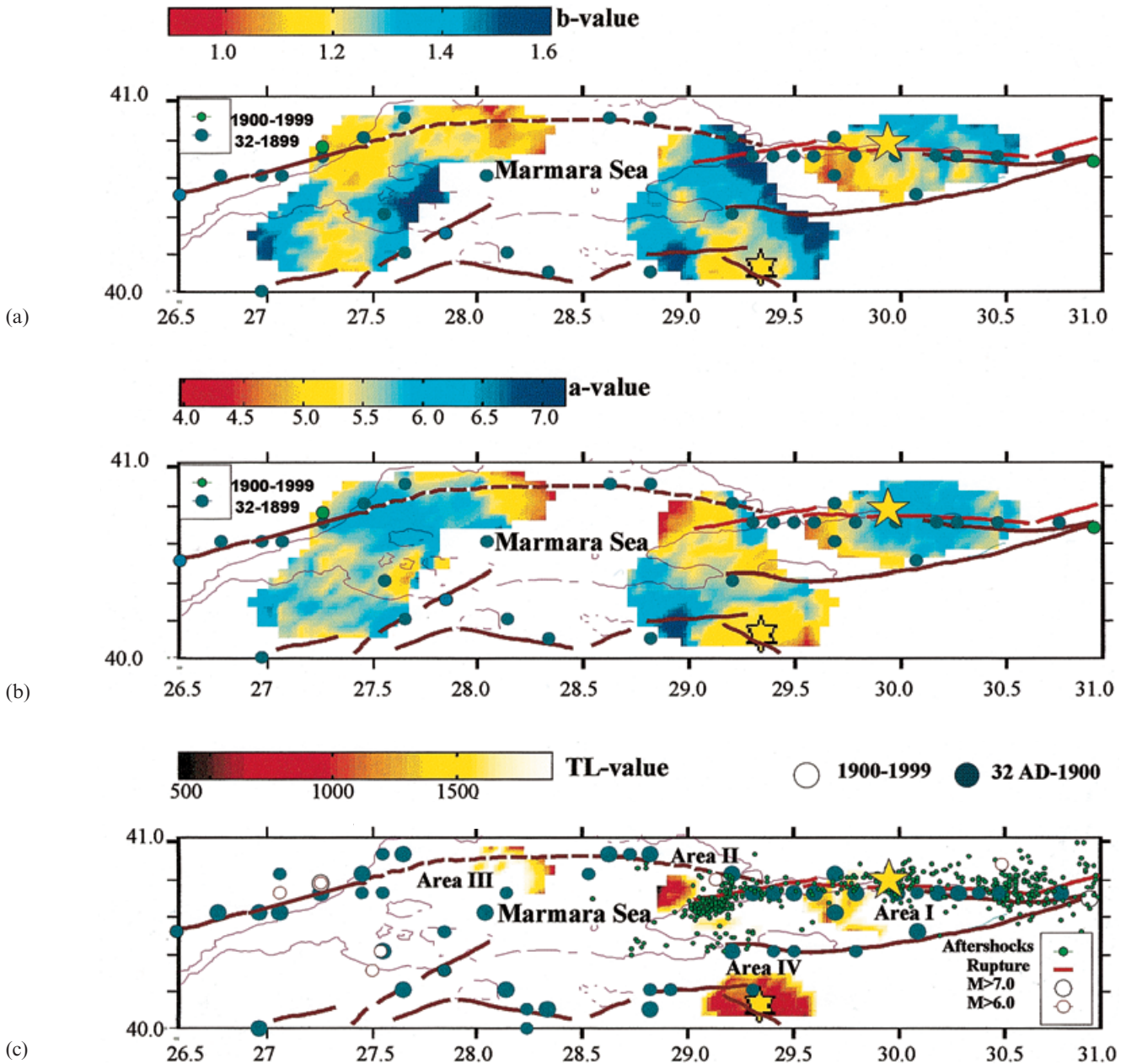
Figure 4. (a) Map of the local *b*-values in the Marmara Sea region and the source volume of the $M_S = 7.4$ Izmit earthquake of August 1999 (star). The node spacing of the grid was 5 km, the radius for sampling earthquakes was 20 km and the minimum number of earthquakes required for an estimate was 50. (b) Map of *a*-values with parameters the same as in (a). Small circles mark the epicentres of 1999 aftershocks, large circles indicate the epicentres of historic earthquakes (Ambraseys & Finkel 1991) for the periods and with the magnitudes indicated in the legend. (c) Map of local recurrence times, T_L, estimated probabilistically for an $M_S = 7.4$ (equal to $M_D = 6.7$) main shock using the *b*- and *a*-values from (a) and (b). Four areas of anomalously short T_L are labelled.

whether any parts of the 1999 Izmit rupture could have been identified as special fault segments before the event, based on the last two decades of seismicity.

We interpret four areas with significantly low *b*-values and anomalously short local recurrence times in the Marmara Sea region as volumes with relatively high stress regimes, i.e. as asperities. Area I in Fig. 4(c) corresponds to the central part of the 1999 rupture zone and includes at its eastern edge the epicentral location of the USGS moment tensor solution. This suggests that the rupture initiated at the edge of an asperity recognizable by the T_L method.

The length of the 1999 aftershock zone in Fig. 4(c) is about 220 km, estimated from the distribution of aftershocks with magnitude $M > 3$ compiled by the Kandilli Observatory. The aftershocks extend from about 29° to 31°, with a strongly active cluster at the western end, at the edge of the anomalous area II (Fig. 4c). The most pronounced part of this T_L anomaly is located to the west of the end of the aftershocks. We interpret this as indicating that the rupture stopped here at an asperity, centred at 28.8°, and did not break though.

The low *b*-values responsible for this anomaly, as well as for the others discussed in the following, are not due to the

incomplete reporting of small events. Not only did we map the threshold value of completeness in terms of earthquake magnitude and cut the catalogue at a conservatively high level of $M_c = 2.9$, but using the ZMAP program we also estimated M_c for every sample in constructing the b- and T_L-maps, using only the data above the local M_c. As a final measure of quality control, we visually check the frequency–magnitude distributions (FMDs) of all areas showing anomalies to be sure that the program's estimates of b and M_c agree with the estimates an observer would obtain manually.

The importance of area II is also underscored by the very local increase of the Coulomb stress change due to a nearby earthquake in 1963 (Plate 1d of Nalbant *et al.* 1998). In addition, the $M4.4$ earthquake of 1999 October 21 (square in Fig. 4), with its five aftershocks, indicates that stresses may be high in area II. The event's magnitude was small but was felt strongly in the Marmara region and especially in Istanbul. It follows that a future rupture along the NAFZ may be likely to initiate at 28.8°E and propagate westwards from there.

The data are too sparse for estimates of T_L in the segment between 28.4° and 28.8°E (Fig. 4c). Several historic main shocks occurred within this low-seismicity segment. Further west than 28.4° we recognize another anomalous volume for T_L, area III (Fig. 4c). This anomaly is located in a segment without historic main-shock epicentres. Nevertheless, we propose that anomaly III may play a significant role in future ruptures. Of course, the representation of a historic $M7$ earthquake by a single point is inadequate in discussing its possible relationship to the potential asperity segments we are trying to map. Thus, we cannot say what role area III may have played in ruptures in the past.

The T_L anomaly in area IV is the only one we found off the northern strand of the NAFZ. It is the most pronounced anomaly of short recurrence times, and the largest earthquake in the data set (an $M5.5$ event in 1983) is located within it (Fig. 4c). Also, this volume is currently seismically quiet at a highly significant statistical confidence level. However, both of these observations, the short T_L and the quiescence, could be due to the 1983 moderate-magnitude earthquake. This earthquake may have increased the seismicity for a few years after it and now the seismicity has returned to a low level that may be normal. Although the location near 40.15°/29.33° attracts attention, we hesitate to interpret this as an indication that a main shock is to be expected, because the observed recent changes can be interpreted as a consequence of the 1983 $M5.5$ earthquake.

We have shown that mapping the b-value, together with estimating the local recurrence time, in the Marmara Sea region has identified the segment of the NAFZ near the centroid location and the western end of the Izmit $M7.4$ earthquake. This identification is based on the roughly two decades of seismicity before the 1999 Izmit event and had no input from the aftershock sequence. Therefore, we suggest that the mapping of T_L provides an important clue for the identification of fault segments that may initiate or stop future large ruptures.

Given the fact that the migration of large earthquakes along the NAFZ from east to west is well established (Ambraseys 1970; Toksöz *et al.* 1979; Barka 1992; Armijo *et al.* 1999), and given that stress coupling was observed between the previous instrumental events in the region (Nalbant *et al.* 1998), we suggest that areas II and III with anomalously short T_L are likely locations for future main shocks, or one rupture that may connect two locations. If the latter should happen then the rupture length would be about 100 km, reaching from about longitude 28° to 29° along the NAFZ in the Marmara Sea.

Since the method of using local recurrence time to map asperities has not yet been extensively tested, our conjectures about the possibility of future earthquakes should be viewed with caution. Also, we have no way of knowing when future events in asperities II, III and IV should be expected.

REFERENCES

Aki, K., 1984. Asperities, barriers, characteristic earthquakes and strong motion prediction, *J. geophys. Res.*, **89**, 5867–5872.

Ambraseys, N.N., 1970. Some characteristic features of the North Anatolian Fault Zone, *Tectonophysics*, **9**, 143–165.

Ambraseys, N.N. & Finkel, C.F., 1991. Long-term seismicity of Istanbul and the Marmara Sea Region, *Terra Nova*, **3**, 527–539.

Amelung, F. & King, G., 1997. Earthquake scaling laws for creeping and non-creeping faults, *Geophys. Res. Lett.*, **24**, 507–510.

Armijo, R., Meyer, B., Hubert, A. & Barka, A., 1999. Westwards propagation of the North Anatolian Fault into the Northern Aegean: timing and kinematics, *Geology*, **27**, 267–270.

Barka, A., 1992. The North Anatolian fault zone, *Ann. Tectonicae*, **6**, 164–195.

Crampin, S. & Üçer, S.B., 1975. The seismicity of the Marmara Sea region of Turkey, *Geophys. J. R. astr. Soc.*, **40**, 269–288.

Frohlich, C. & Davis, S., 1993. Teleseismic b-values: or, much ado about 1.0, *J. geophys. Res.*, **98**, 631–644.

Kagan, Y.Y. & Jackson, D.D., 1991. Long-term earthquake clustering, *Geophys. J. Int.*, **104**, 117–133.

Lay, T., Kanamori, H. & Ruff, L., 1982. The asperity model and the nature of large subduction zone earthquakes, *Earthq. Pred. Res.*, **1**, 3–72.

Mogi, K., 1962. Magnitude-frequency relation for elastic shocks accompanying fractures of various materials and some related problems in earthquakes, *Bull. Earthq. Res. Inst. Univ. Tokyo*, **40**, 831–853.

Nalbant, S., Hubert, A. & King, G., 1998. Stress coupling between earthquakes in northwest Turkey and the north Aegean sea, *J. geophys. Res.*, **103**, 24 469–24 486.

Ogata, Y. & Katsura, K., 1993. Analysis of temporal and spatial heterogeneity of magnitude frequency distribution inferred from earthquake catalogues, *Geophys. J. Int.*, **113**, 727–738.

Öncel, A.O. & Alptekin, Ö., 1995. Earthquake risk in Marmara Sea, *Proc. Turkish National Union of Geodesy and Geophysics, General Assembly*, **3**, 981–989.

Öncel, A.O. & Alptekin, Ö., 1999a. Effect of aftershocks on earthquake hazard estimation: an example from the north Anatolian fault zone, *Natural Hazards*, **19**, 1–11.

Öncel, A.O. & Alptekin, Ö., 1999b. *Microseismicity and Seismic Hazard of Marmara Region*, Project 1038/250897, Istanbul University, Istanbul, Turkey.

Öncel, A.O., Alptekin, Ö. & Main, I., 1995. Temporal variations of the fractal properties of seismicity in the western part of the north Anatolian fault zone: possible artefacts due to improvements in station coverage, *Nonlinear Proc. Geophys.*, **2**, 147–157.

Öncel, A.O., Main, I., Alptekin, Ö. & Cowie, P., 1996a. Spatial variations of the fractal properties of seismicity in the Anatolian Fault Zones, *Tectonophysics*, **257**, 189–202.

Öncel, A.O., Main, I., Alptekin, Ö. & Cowie, P., 1996b. Temporal variations of the fractal properties of seismicity in the north Anatolian fault zone between 31°E and 41°E, *Pure appl. Geophys.,* **146,** 147–159.

Öncel, A.O., Wilson, H.T. & Nishizawa, O., 1999. Size scaling relationships in the active fault networks of Japan and their correlation with Gutenberg-Richter b values, *J. geophys. Res.,* submitted.

Reasenberg, P.A., 1985. Second-order moment of Central California seismicity, *J. geophys. Res.,* **90,** 5479–5495.

Scholz, C.H., 1968. The frequency-magnitude relation of microfracturing in rock and its relation to earthquakes, *Bull. seism. Soc. Am.,* **58,** 399–415.

Straub, C. & Kahle, H., 1995. Active crustal deformation in the Marmara Sea Region, NW Anatolia, inferred from GPS measurements, *Geophys. Res. Lett.,* **22,** 2533–2536.

Toksöz, M.N., Shakal, A.F. & Michael, A.J., 1979. Space-time migration of earthquakes along the North Anatolian fault zone and seismicity gaps, *Pageoph,* **117,** 1258–1270.

Urbancic, T.I., Trifu, C.I., Long, J.M. & Young, R.P., 1992. Space-time correlations of b-values with stress release, *Pageoph,* **139,** 449–462.

Warren, N.W. & Latham, G.V., 1970. An experimental study of thermally induced microfracturing and its relation to volcanic seismicity, *J. geophys. Res.,* **75,** 4455–4464.

Wiemer, S., 1996. Analysis of seismicity: new techniques and case studies, *Dissertation thesis,* University of Alaska, Fairbanks, Alaska.

Wiemer, S. & Benoit, J., 1996. Mapping the b-value anomaly at 100 km depth in the Alaska and New Zealand subduction zones, *Geophys. Res. Lett.,* **23,** 1557–1560.

Wiemer, S. & McNutt, S., 1997. Variations in frequency-magnitude distribution with depth in two volcanic areas: Mount St. Helens, Washington, and Mt. Spurr, Alaska, *Geophys. Res. Lett.,* **24,** 189–192.

Wiemer, S. & Wyss, M., 1997. Mapping the frequency-magnitude distribution in asperities: an improved technique to calculate recurrence times?, *J. geophys. Res.,* **102,** 15 115–15 128.

Wyss, M., 1973. Towards a physical understanding of the earthquake frequency distribution, *Geophys. J. R. astr. Soc.,* **31,** 341–359.

Wyss, M. & Brune, J.N., 1967. The Alaska earthquake of 28 March 1964: a complex multiple rupture, *Bull. seism. Soc. Am.,* **81,** 1231–1254.

Wyss, M. & Wiemer, S., 1997. Two current seismic quiescences within 40 km of Tokyo, *Geophys. J. Int.,* **128,** 459–473.

Wyss, M., Schorlemmer, D. & Wiemer, S., 2000. Mapping asperities by minima of local recurrence time: the San Jacinto-Elsinore fault zones, *J. geophys. Res.,* **105,** 7829–7844.

Zuniga, R. & Wyss, M., 2000. Most and least likely locations of large to great earthquakes along the Pacific Coast of Mexico, estimated from local recurrence times based on *b*-values, *J. geophys. Res.,* **103,** in press.